# Sterile neutrino study by new schemes for low-energy neutrino sources by accelerator and non-accelerator

**Myung-Ki Cheoun**, J. Shin, Heamin Ko, Dukjae Jang
(Soongsil Univ., Seoul)
T. Hayakawa (JAEA), T. Kajino (NAOJ) …
G. Mathews (Nortre Dame), B. Ballantekin (Wisconsin),
M. Kusakabe (Beihang), P. Yamac (Minmar) …

KPS Fall Meeting
25 Oct. – 27 Oct., 2017
Kyungju, Korea

# Contents

- Neutrino Anomaly and Sterile Neutrino
- Sterile Neutrino in the early Universe, BBN, and Supernova Explosion
- Low Energy Neutrino Source Schemes
- By Accelerator
- By Non-Accelerator
- Summary

# However, Four Experimental Anomalies Do Not Fit Within the 3ν Mixing Picture

- LSND
- MiniBooNE
- The Gallium Anomaly
- The Short Base-Line Reactor Neutrino Anomaly

**These anomalies possibly suggest a fourth sterile neutrino, requiring a mass on the 1 eV scale.**

**However, there are also complex nuclear physics issues associated with each anomaly.**

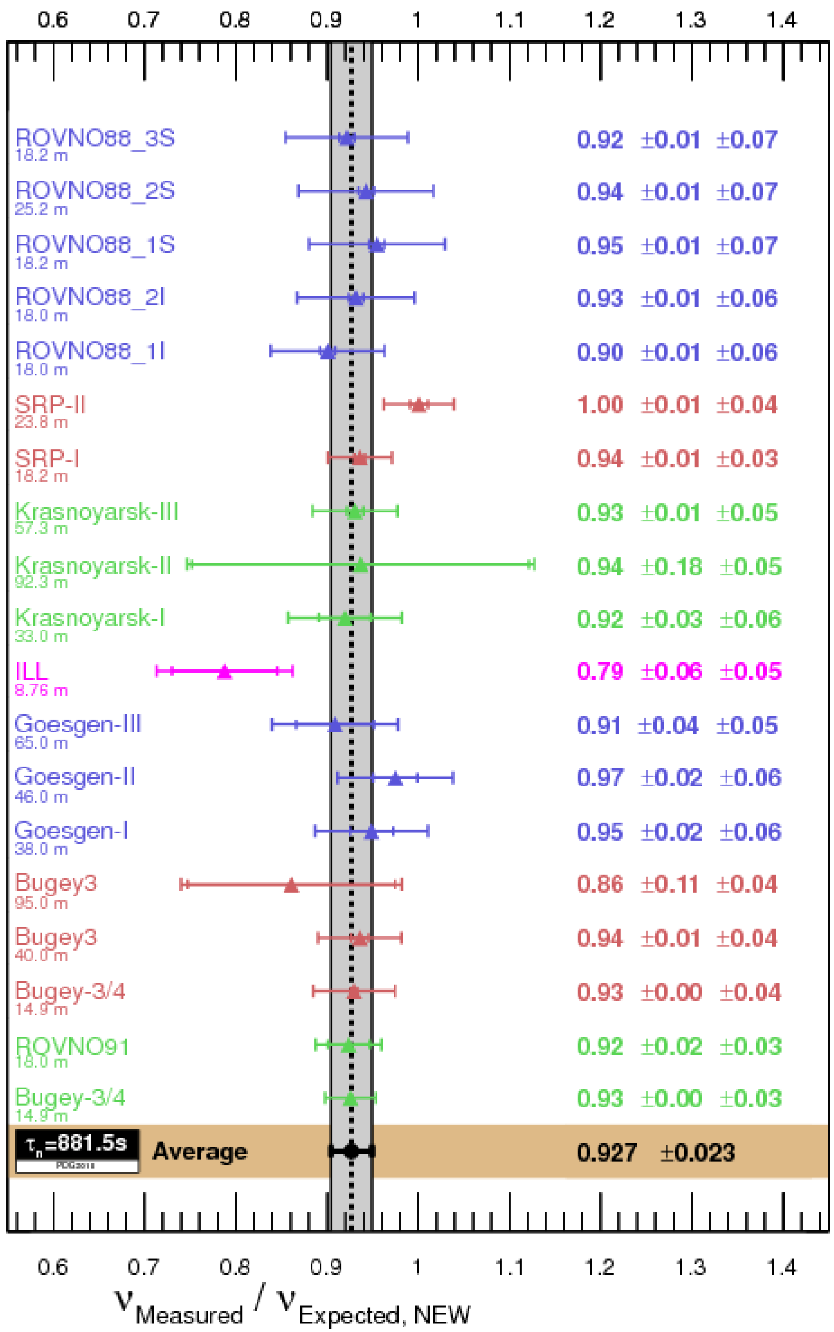


Weighted average (with correlations) of 19~measurements of reactor neutrino experiments operating at short baselines. A summary of experiment details is given in Table~???

# Contents

- **Neutrino Anomaly and Sterile Neutrino**
- **Sterile Neutrino in the early Universe, BBN, and Supernova Explosion**
- **Low Energy Neutrino Source Schemes**
- **By Accelerator**
- **By Non-Accelerator**
- Summary

# How to understand the origin of Sterile Neutrino ?

Among many scenarios of the sterile neutrino, Päs *et al.* [6] assumed that the sterile neutrino is a gauge-singlet particle and can travel on or off our 3 + 1 dimensional brane embedded in a large extra dimension bulk similarly to the graviton in the brane-world cosmology. According to the cosmology, ordinary matter fields are confined to a three-dimensional space in the high dimensional bulk. Originally, the brane-world cosmology was suggested to explain the hierarchy problem, the large scale difference between the standard model force and the gravity [7, 8]. Randall and Sundrum suggested a new solution of the hierarchy problem by introducing noncompact extra dimensions [9, 10]. Ref. [6] suggested a model, in which a sterile neutrino can propagate in the bulk and brane similarly to the graviton. They derived a new formula of resonant active-sterile neutrino oscillation and found an allowed region of the resonance energy from the comparison to available experimental data.

# Sterile-active neutrino oscillations and shortcuts in the extra dimension

[H. pas et al., Phys. Rev. D **72**, 095017 (2005)]

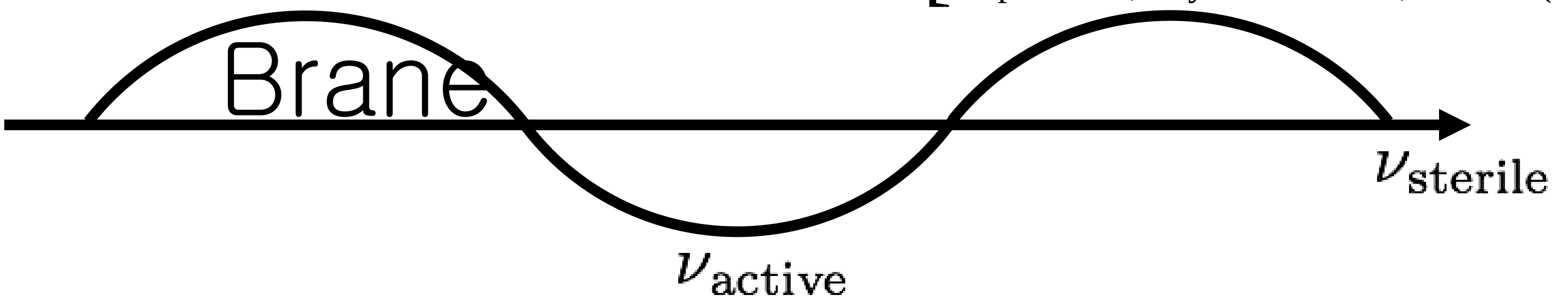


**How does it affect the big bang nucleosynthesis?**

PHYSICAL REVIEW D **94**, 113010 (2016)

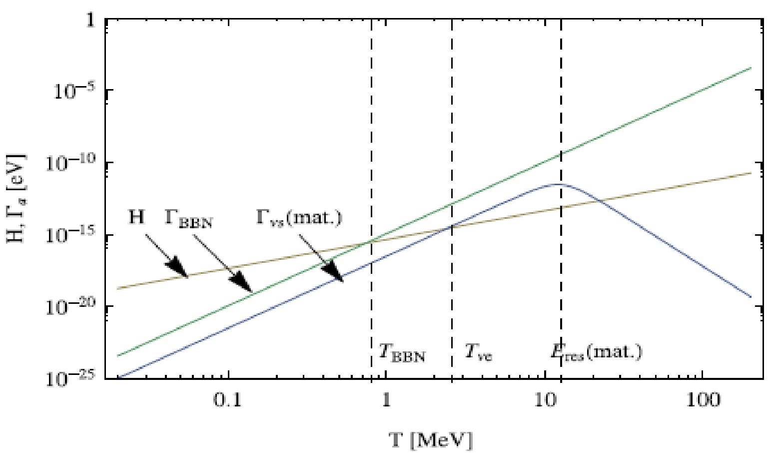


FIG. 1. Reaction rates $\Gamma_{\text{BBN}}$, $\Gamma_{\nu_s}$ as a function of temperature in comparison with the Hubble rate $H$. BBN happens where $\Gamma_{\text{BBN}}$ falls below the Hubble rate. $\Gamma_{\nu_s}$ denotes the reaction rate of sterile neutrinos with a matter potential for $\nu_e - \nu_s$ oscillations with $\sin^2\theta = 0.03$, $\Delta m^2 = 0.93$ eV$^2$.

$$\Gamma_{\nu_s} = \langle P_{\nu_a \to \nu_s} \rangle \Gamma_{\nu_a}.$$

$$\langle P_{\nu_a \to \nu_s} \rangle = \left\langle \sin^2\left(\frac{\Delta\mathcal{H}}{2} t\right) \sin^2(2\tilde{\theta}) \right\rangle = \frac{1}{2}\sin^2(2\tilde{\theta}),$$

$$\Gamma_{\nu_s}(T) \lesssim H(T)$$

# The cosmic expansion rate in five-dimensional universe

$$H^2 = \frac{8\pi G}{3}\rho + \frac{\mathcal{E}}{a^4}$$

P. Binetrun *et* al., Phys. Lett. B **477**, 285 (2000)

$a$ : scale factor

$\rho$ : energy density

$G$ : Gravitational constant

$\mathcal{E}$ : integration constant

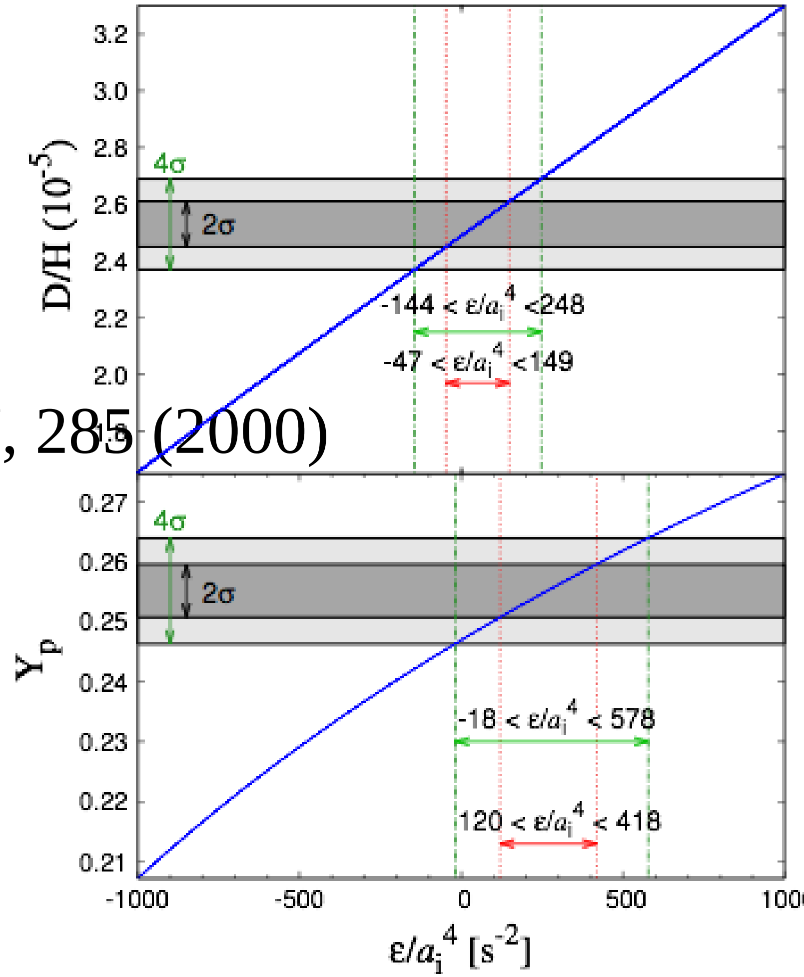


D/H : R. Cooke *et* al., Astrophys. J. **781**, 31 (2014)

Yp : Y. I. Izotov *et* al., Astron. Soc. **445**, 778 (2014)

# The energy density of the sterile neutrino

$$\rho = \rho_{\mathrm{standard}} + \rho_{\nu_s}$$

## Rate equation

$$\frac{x}{Y_{\mathrm{EQ}}}\frac{dY_{\nu_s}}{dx} = -\frac{\Gamma_{\nu_s}}{H}\left[\left(\frac{Y_{\nu_s}}{Y_{\mathrm{EQ}}}\right)^2 - 1\right]$$

$x : m_{\nu_s}/T$ $\quad Y = n/s$ $\quad n$ : number density

$Y_{\mathrm{EQ}} = n_{\mathrm{EQ}}/s$ $\quad s$ : entropy density

The production rate of the sterile neutrino:

$$\Gamma_{\nu_s} = P_{\mathrm{as}}\langle\Gamma_{\mathrm{weak}}\rangle$$

$$P_{\mathrm{as}} = \begin{cases} \sin^2 2\tilde{\theta}\sin^2\left(\frac{\delta m^2_{\mathrm{mat}} t_{\mathrm{sc}}}{4E}\right), & (\text{for } T \geq T_{\mathrm{EQ}}) \\ \frac{1}{2}\sin^2 2\tilde{\theta}, & (\text{for } T \leq T_{\mathrm{EQ}}) \end{cases}$$

$$\langle\Gamma_{\mathrm{weak}}\rangle \to \Gamma_{\tau} = 2.9 G_F^2 T^5 \ (\nu_\tau \text{ and } \nu_{\mathrm{s}})$$

# The effective mixing angle

$$\sin^2 2\tilde{\theta} = \frac{\sin^2 2\theta}{\sin^2 2\theta + \cos^2 2\theta \left[ 1 + \underbrace{\frac{C_\alpha G_F^2 T^4 E^2}{\cos 2\theta \alpha \delta m^2}}_{\text{Matter effect}} - \underbrace{\left( \frac{E}{E_{\mathrm{res}}} \right)^2}_{\text{Geodesic differences between bulk and brane}} \right]^2}$$

$\theta$ : bare mixing angle between $\nu_{\mathrm{s}}$ and $\nu_{\mathrm{a}}$ $\qquad$ $C_e = 1.22, \; C_{\mu,\tau} = 0.34$

$\delta m^2$ : mass squared differences $\qquad$ $E = 3.151 \, T_{\nu_s}$

# Resonance energy

$$E_{\mathrm{res}} = \sqrt{\frac{\delta m^2 \cos 2\theta}{2\epsilon_s}} \qquad \epsilon_s = \frac{(D_{\mathrm{brane}} - D_{\mathrm{bulk}})}{D_{\mathrm{brane}}} \qquad D : \text{geodesic}$$

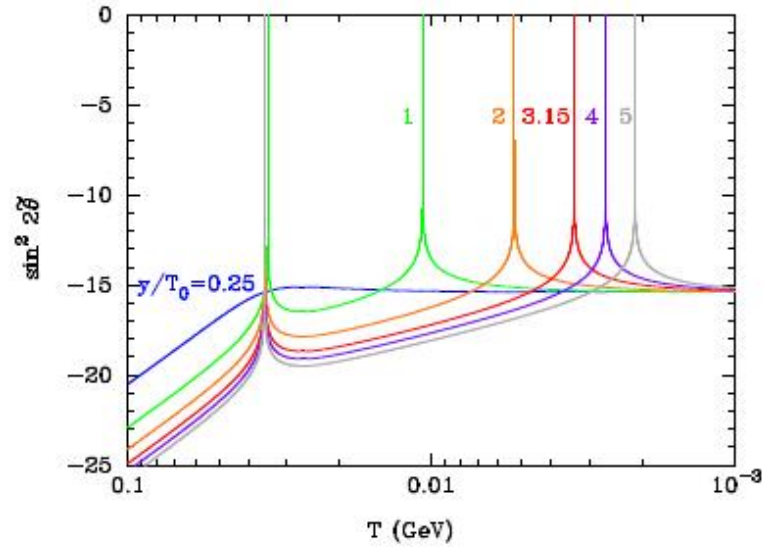


FIG. 15. (Color online) The effective mixing angle as a function of temperature for $y/T_0 = 0.25$, 1, 2, 3.15, 4, and 5. Adopted parameters are the same as in Fig 14.

# The result of the rate equation $(Y_{\nu_s} = n_{\nu_s}/s)$

Contour

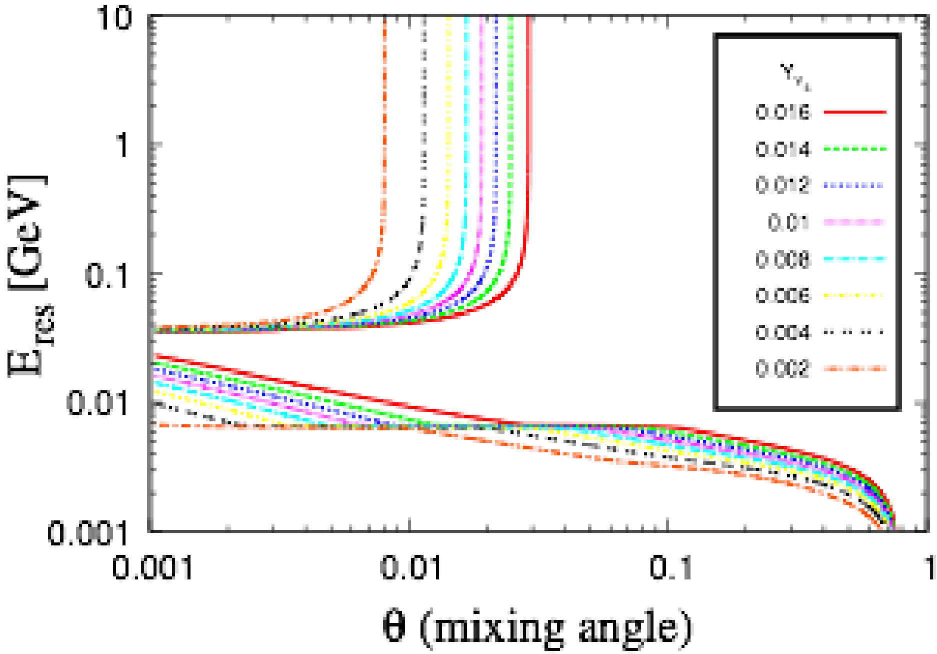


$$\rho_{\nu_s} = \begin{cases} n_{\nu_s} \langle E_{\nu_s} \rangle , & \text{for a relativistic case} \\ n_{\nu_s} m_{\nu_s} , & \text{for a non-relativistic case} \end{cases}$$

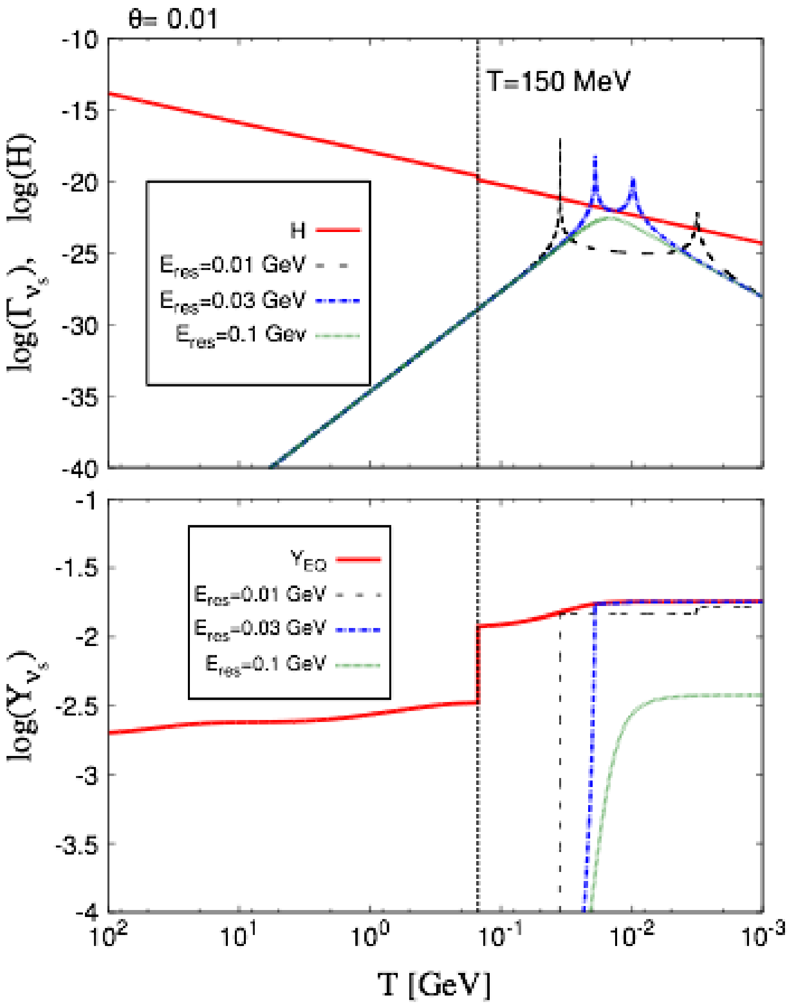


Temperature evolution

# BBN constraint

$$(\theta, \delta m^2 E_{\rm res}, \mathcal{E}) \longrightarrow \rho_{\nu_s} \longrightarrow H \longrightarrow \mathrm{D/H,\ Y_p}$$

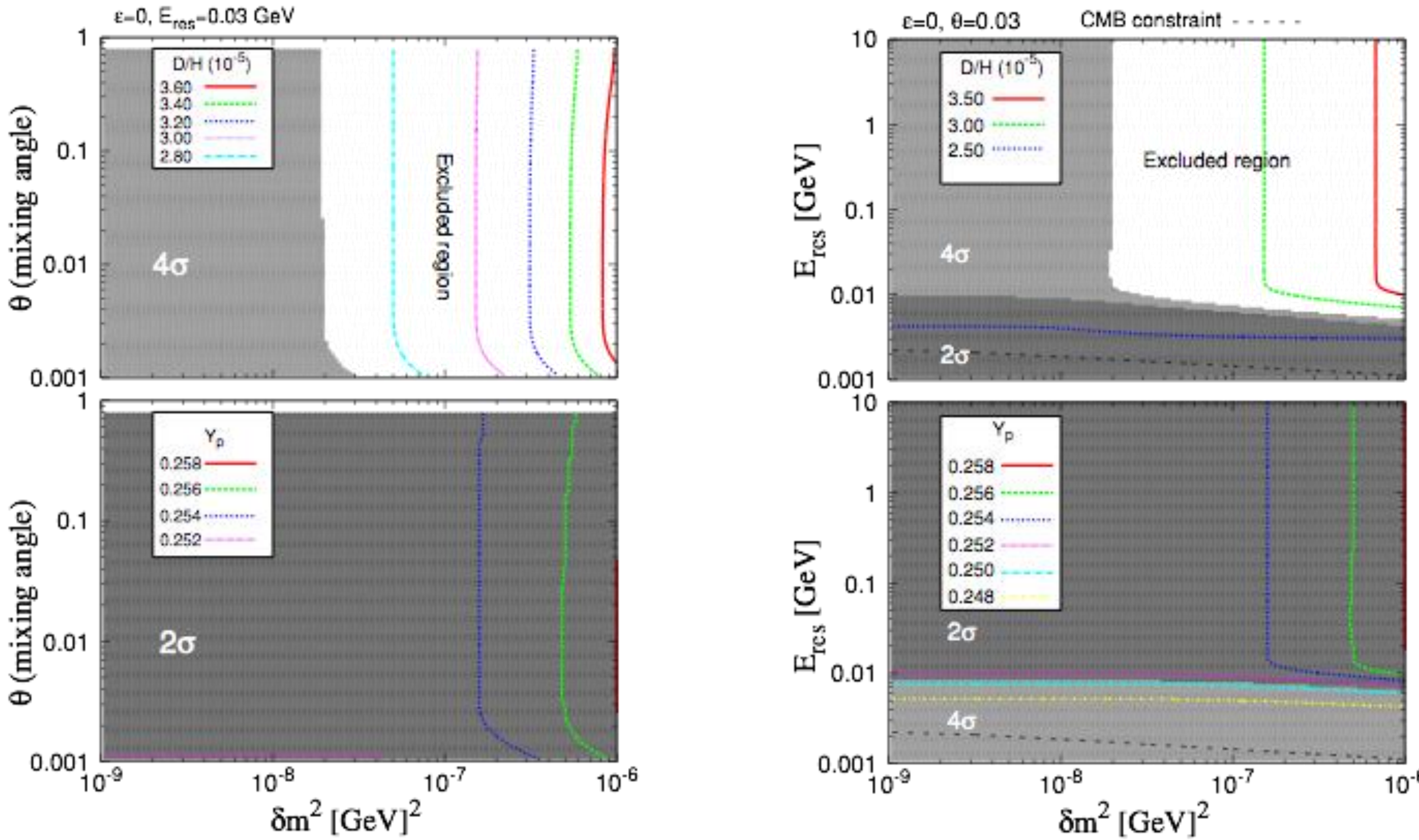

We showed a result of a parameter search in the plane of $(\theta,\, m_{\nu_s})$ for a fixed $E_{\rm res}$ value. We found that the region of $m_{\nu_s} \gtrsim \mathcal{O}(10^{-4})$ GeV is excluded within all mixing angle parameter space searched in this study when $E_{\rm res} = 0.03$ GeV. On the other hand, all mixing angle parameter space are allowed when $m_{\nu_s} \lesssim \mathcal{O}(10^{-4})$ GeV within $4\,\sigma$ range. This is because the heavier mass leads

# Contents

- Neutrino Anomaly and Sterile Neutrino
- Sterile Neutrino in the early Universe, BBN, and Supernova Explosion
- Low Energy Neutrino Source Schemes
- By Accelerator
- By Non-Accelerator
- Summary

# CC Supernova Explosion

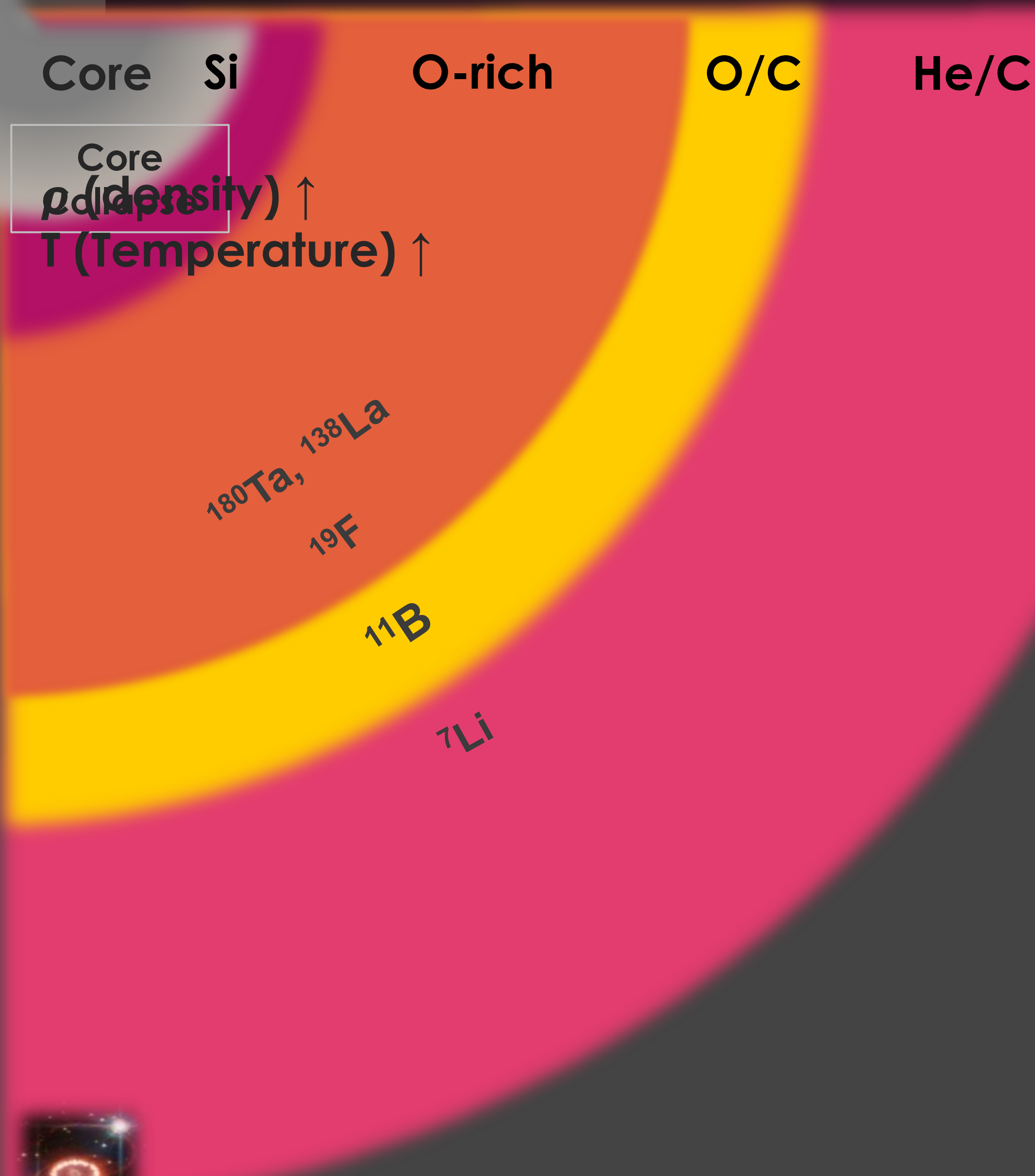


**Electron flavor ($\nu_e$ and $\bar{\nu}_e$)**

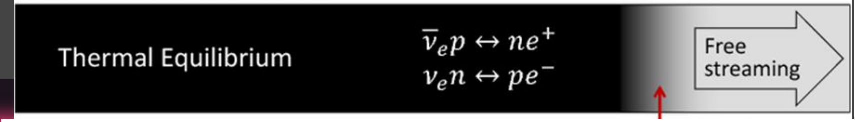


TABLE 25

SUMMARY TABLE: SPECIES DUE TO NEUTRINO NUCLEOSYNTHESIS[a]

| Species | H | He | C | Ne | O | NSE |
|---|---|---|---|---|---|---|
| $^{7}$Li | B | A | C | ... | ... | A |
| $^{10}$B | ... | C | B | ... | ... | ... |
| $^{11}$B | ... | B | A | ... | ... | A |
| $^{15}$N | ... | ... | C | C | C | ... |
| $^{19}$F | ... | ... | ... | A | ... | ... |
| $^{22}$Na | ... | ... | ... | E | ... | ... |
| $^{26}$Al | ... | ... | ... | E | ... | ... |
| $^{27}$Al | ... | ... | ... | ... | C | ... |
| $^{31}$P | ... | ... | ... | ... | E | ... |
| $^{35}$Cl | ... | ... | ... | E | E | ... |
| $^{39}$K | ... | ... | ... | ... | E | ... |
| $^{40}$K | ... | ... | ... | E | B | ... |
| $^{41}$K | ... | ... | ... | ... | E | ... |
| $^{43}$Ca | ... | ... | ... | C | C | ... |
| $^{45}$Sc | ... | ... | ... | ... | C | B |
| $^{47}$Ti | ... | ... | ... | C | C | C |
| $^{49}$Ti | ... | ... | ... | ... | ... | B |
| $^{50}$V | ... | ... | ... | E | B | B |
| $^{51}$V | ... | ... | ... | C | E | E |
| $^{55}$Mn | ... | ... | ... | ... | ... | E |
| $^{59}$Co | ... | ... | ... | ... | ... | E |
| $^{63}$Cu | ... | ... | ... | ... | ... | B |
| $^{138}$La | ... | ... | ... | A | ... | ... |
| $^{180}$Ta | ... | ... | ... | A | ... | ... |

[a] A = species produced in full abundance; B = important production; C = minor production; E = enhanced significant production.

Woosley, S. E., Hartmann, D. H., Hoffman, R. D., & Haxton, W. C. 1990, ApJ, 356, 272

# The production of $^{98}$Tc in $\nu-$process

$$^{98}\mathrm{Mo} + \nu_e \rightarrow {}^{98}\mathrm{Tc}^* + e^- \rightarrow {}^{98}\ \mathrm{Tc}$$
$$^{99}\mathrm{Ru} + \nu_{e,\mu}(\bar{\nu}_{e,\mu}) \rightarrow {}^{99}\mathrm{Ru}^* + \nu'_{e,\mu}(\bar{\nu}'_{e,\mu}) \rightarrow {}^{98}\mathrm{Tc} + p$$

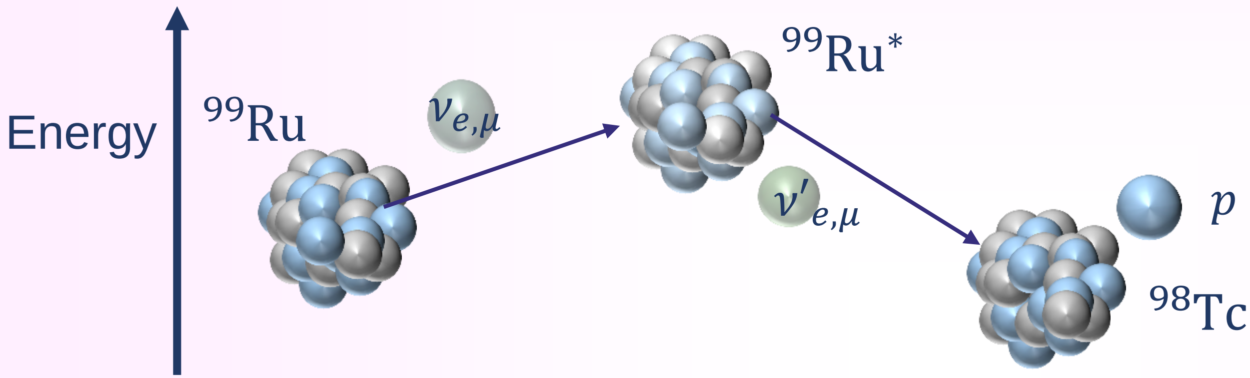


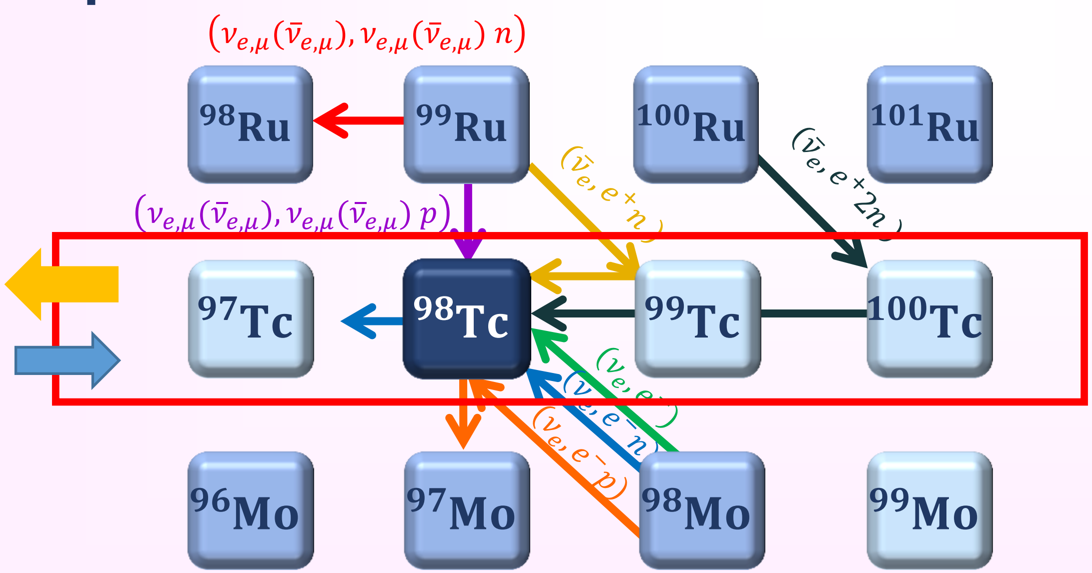


$^{99}\mathrm{Ru}(\bar{\nu}_e, \bar{\nu}_e n)^{98}\mathrm{Ru}$
$^{99}\mathrm{Ru}(\bar{\nu}_\mu, \bar{\nu}_\mu n)^{98}\mathrm{Ru}$
$^{99}\mathrm{Ru}(\nu_e, \nu_e\ n)^{98}\mathrm{Ru}$
$^{99}\mathrm{Ru}(\nu_\mu, \nu_\mu\ n)^{98}\mathrm{Ru}$

$^{99}\mathrm{Ru}(\bar{\nu}_e, \bar{\nu}_e p)^{98}\mathrm{Tc}$
$^{99}\mathrm{Ru}(\bar{\nu}_\mu, \bar{\nu}_\mu p)^{98}\mathrm{Tc}$
$^{99}\mathrm{Ru}(\nu_e, \nu_e\ p)^{98}\mathrm{Tc}$
$^{99}\mathrm{Ru}(\nu_\mu, \nu_\mu\ p)^{98}\mathrm{Tc}$

$^{98}\mathrm{Mo}(\nu_e, e^- n)^{97}\mathrm{Tc}$

$^{98}\mathrm{Mo}(\nu_e, e^- p)^{97}\mathrm{Mo}$

$^{98}\mathrm{Mo}(\nu_e, e^-)^{98}\mathrm{Tc}$

$^{99}\mathrm{Ru}(\bar{\nu}_e, e^+ n\ )^{98}\mathrm{Tc}$

$^{100}\mathrm{Ru}(\bar{\nu}_e, e^+ 2n\ )^{98}\mathrm{Tc}$

M.K. Cheoun, et al., Phys.Rev. C.85. 065807 (2012)

# Neutrino Spectra and sensitivity for nucleosyntheses

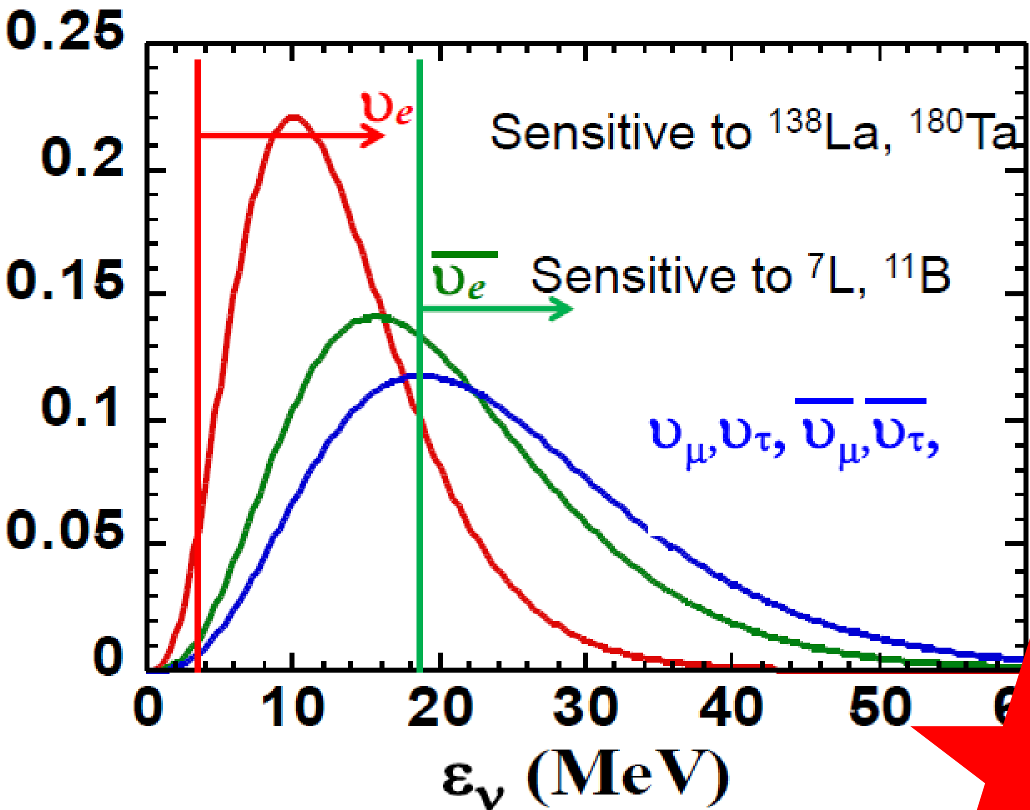


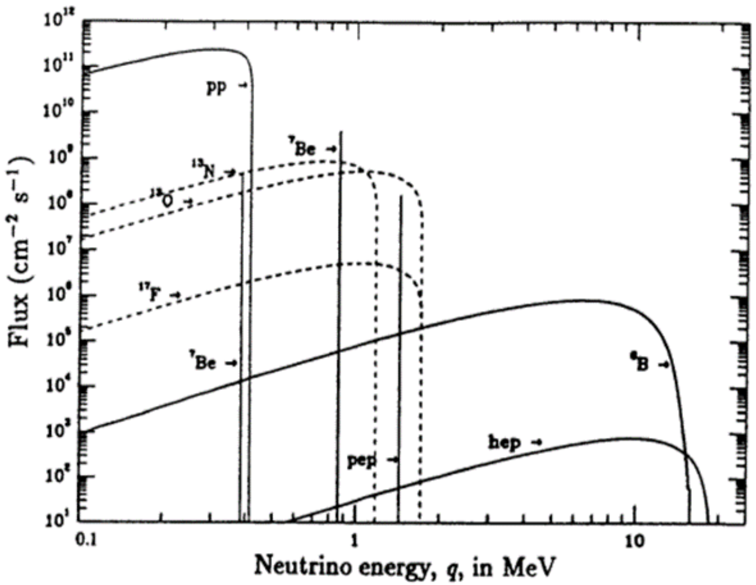


Fig. 44. Solar neutrino spectrum. Energy spectrum of solar neutrinos, as predicted by the standard sola model. Solid and dashed curves distinguish between neutrinos produced in the pp-chains and the CNO cycle respectively. (From 49.)

# Nuclear chart simulation

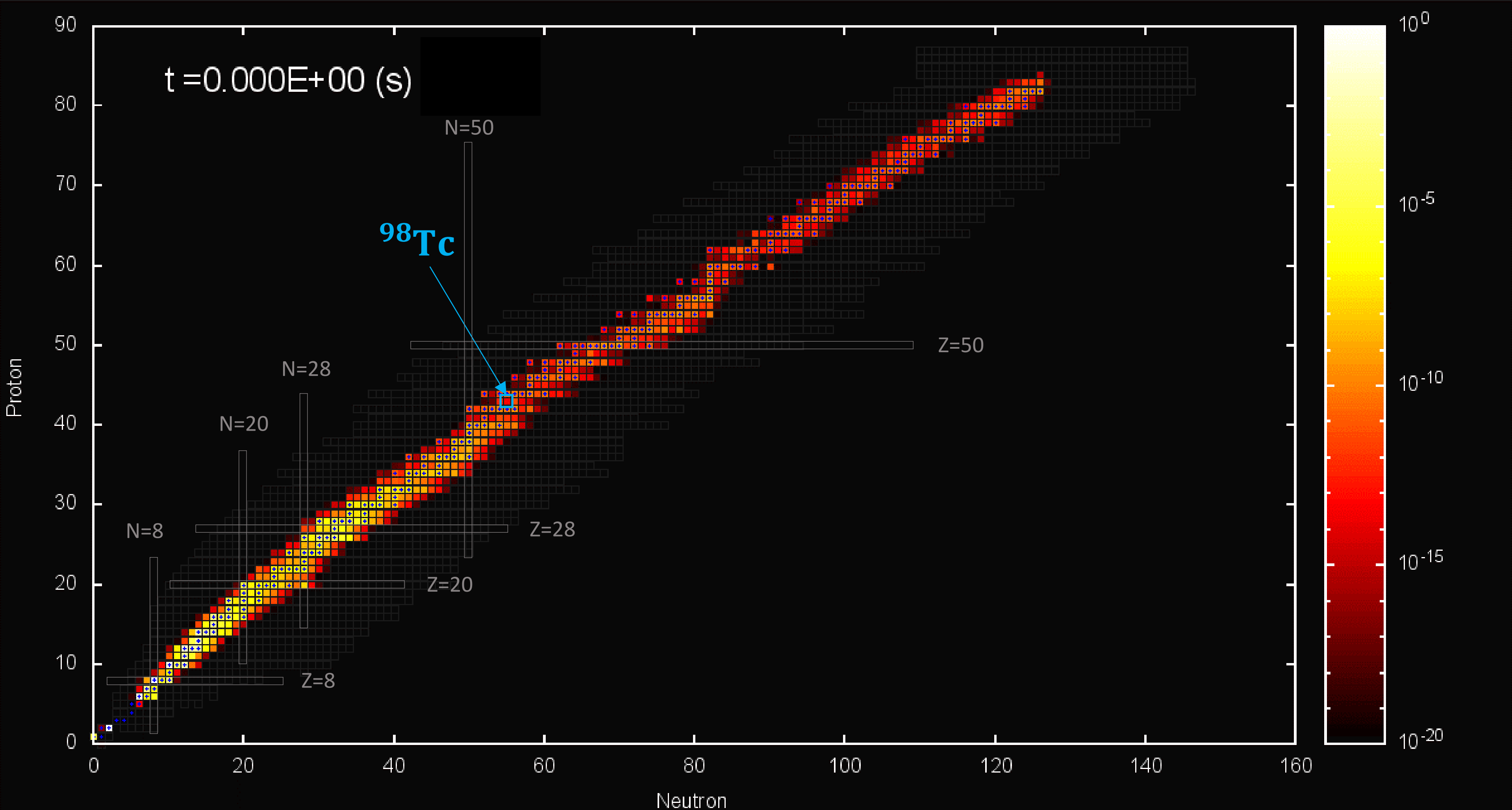


**Middle of O-rich ~ He/C layer (2.4 ~ 6 $M_{\odot}$)**

# Result – total abundance

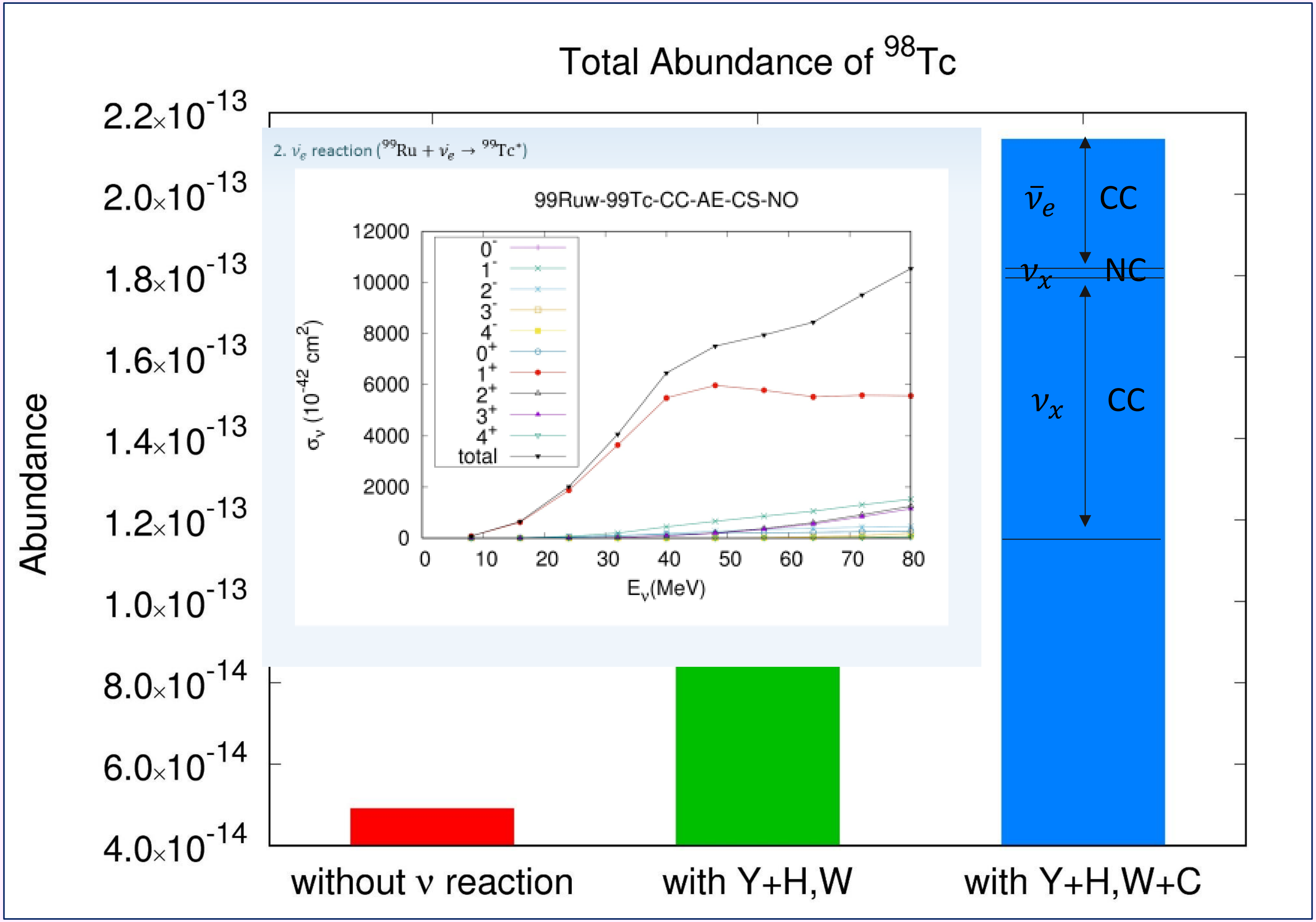

# ν-reaction (2 step) Data in Low E. region: KARMEN/LSND/CC and NC

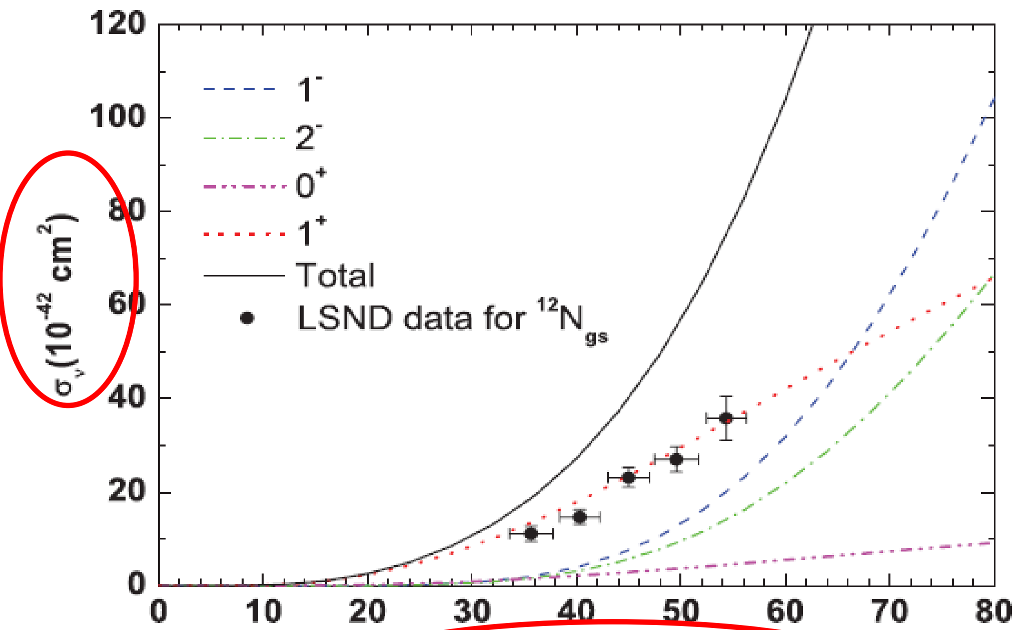


LSND : $\nu_e$ $^{12}C \rightarrow e^- + {}^{12}N^*$ $(1^+)$

PHYSICAL REVIEW C, VOLUME 64, 065501

**Measurements of charged current reactions of $\nu_e$ on $^{12}C$**

L. B. Auerbach,[8] R. L. Burman,[5] D. O. Caldwell,[3] E. D. Church,[1] J. B. Donahue,[5] A. Fazely,[7] G. T. Gar
R. M. Gunasingha,[7] R. Imlay,[6] W. C. Louis,[5] R. Majkic,[8] A. Malik,[6] W. Metcalf,[6] G. B. Mills,[5] V. Sandberg,[5] I
I. Stancu,[1,*] M. Sung,[6] R. Tayloe,[5,†] G. J. VanDalen,[1] W. Vernon,[2] N. Wadia,[6] D. H. White,[5] and S. Yel

Table 1. Flux-averaged cross sections for neutrinos from $\pi^+$ and $\mu^+$ DAR, measured with KARMEN1 (K1) and KARMEN2 (K2).

| Reaction | $\langle\sigma\rangle$ in $10^{-42}$ cm$^2$ | Comment |
|---|---|---|
| $^{12}C\ (\nu_e, e^-)\ ^{12}N_{g.s.}$ | $9.6 \pm 0.3_{(stat)} \pm 0.7_{(syst)}$ | 846 sequences in K1 and K2 |
| $^{12}C\ (\nu, \nu')\ ^{12}C^*$ | $10.2 \pm 0.4_{(stat)} \pm 0.8_{(syst)}$ | $\nu = \nu_e, \bar{\nu}_\mu$, K1 and K2 |
| $^{12}C\ (\nu, \nu')\ ^{12}C^*$ | $3.2 \pm 0.5_{(stat)} \pm 0.4_{(syst)}$ | $\nu = \nu_\mu$, data from K1 only |
| $^{12}C\ (\nu_e, e^-)\ ^{12}N^*$ | $4.8 \pm 0.6_{(stat)}\ ^{+0.4}_{-0.5}{}_{(syst)}$ | $\chi^2$-fit on energy spectrum of K2 |
| $^{13}C\ (\nu_e, e^-)\ ^{13}N$ | $50 \pm 25_{(stat)}\ ^{+4}_{-6}{}_{(syst)}$ | K2 special window evaluation |
| $^{56}Fe\ (\nu_e, e^-)\ X$ | $217 \pm 135_{(stat)}\ ^{+27}_{-65}{}_{(syst)}$ | $\chi^2$-fit on energy spectrum of K2 |

JSNS^2 at JPARC

# Conclusion and Outlook

In reality,
we do not have direct data !!

Only a few data limited to C
for a specific channel

Should we believe the estimation
of neutrino reactions and scattering ?

No way, believe in nuclear theory !!

For the r-process nuclei,
Lots of data with extensive and intensive
discussions have been accumulated !!

Needs lots of discussions !!!

How to justify theoretical estimation
from existing nuclear reaction data ?

Partially, GT for CC and M1 spin
transitions
for NC reactions.

**need high intense proton beam or**
**ng neutron emitter.**

# Contents

PHYSICAL REVIEW C 94, 045804 (2016)

New neutrino source for the study of solar neutrino physics in the vacuum-matter transition region

Journal of Cosmology and Astroparticle Physics
An IOP and SISSA journal

Short-baseline electron antineutrino disappearance study by using neutrino sources from $^{13}$C + $^{9}$Be reaction

Jae Won Shin,[a] Myung-Ki Cheoun,[a,1] Toshitaka Kajino[b,c]
and Takehito Hayakawa[d]

Letters

IOP Publishing
Journal of Physics G: Nuclear and Particle Physics

J. Phys. G: Nucl. Part. Phys. 44 (2017) 09LT01 (10pp)
https://doi.org/10.1088/1361-6471/aa809e

Letter

A new scheme for short baseline electron antineutrino disappearance study

Jae Won Shin[1], Myung-Ki Cheoun[1], Toshitaka Kajino[2,3] and Takehito Hayakawa[4]

# The accelerator-based IsoDAR concept

✓ If we scatter the **proton accelerator beam of 15 MeV and 10 mA off the $^{27}$Al target**, we obtain **3.55×10$^{13}$ $^{27}$Si isotope per second** according to JENDL-4.0/HE data.

## 1. $^{27}$Si production setup

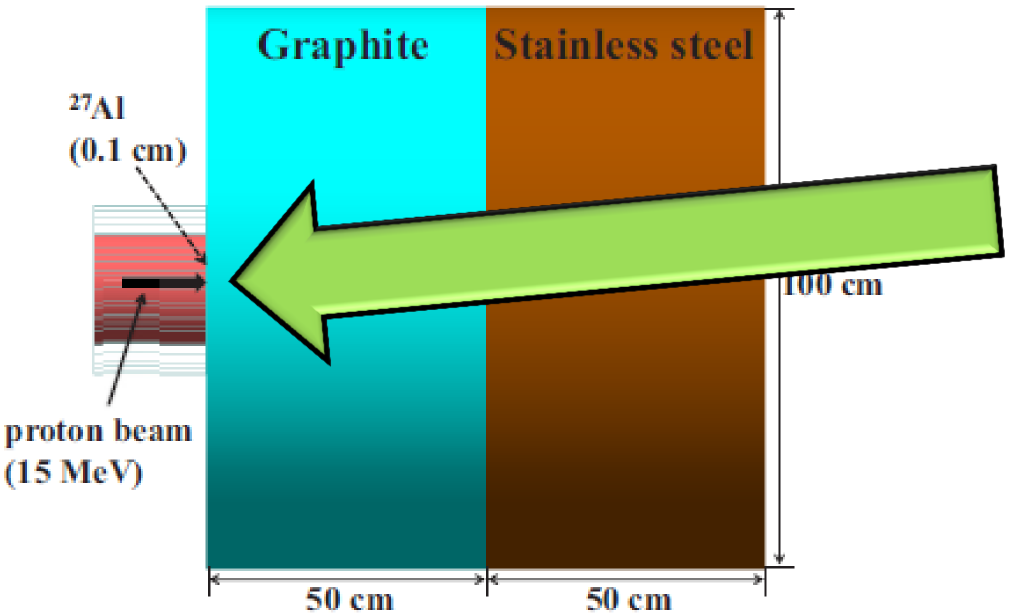


***Schematic diagram of the simulation geometry***

| | |
|---|---|
| $^{27}$Al | : $^{27}$Si production target (0.1 mm × 10 layers) |
| N-gas | : cooling |
| Graphite | : proton stopper, neutron shielding, heat |
| Polystyrene | : neutron shielding, g shielding |

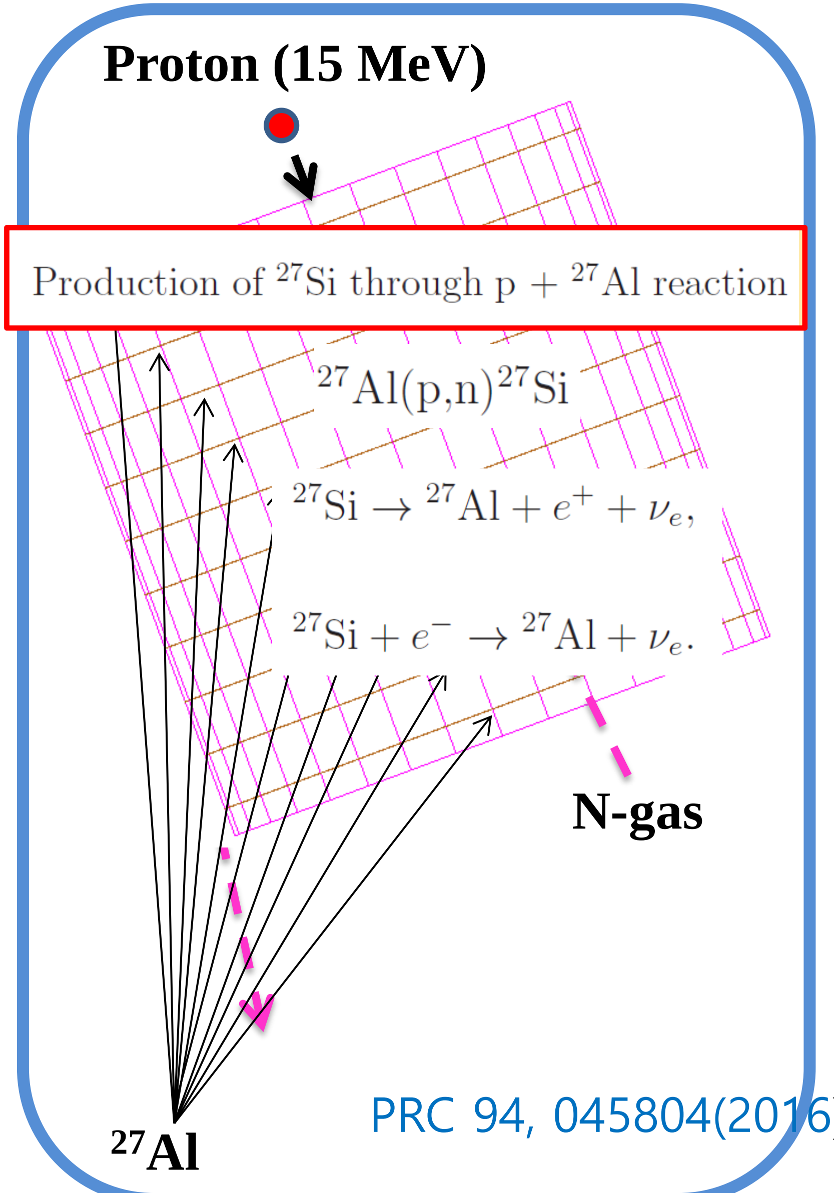

## 2. Results

### 2.1. Radiochemical detectors

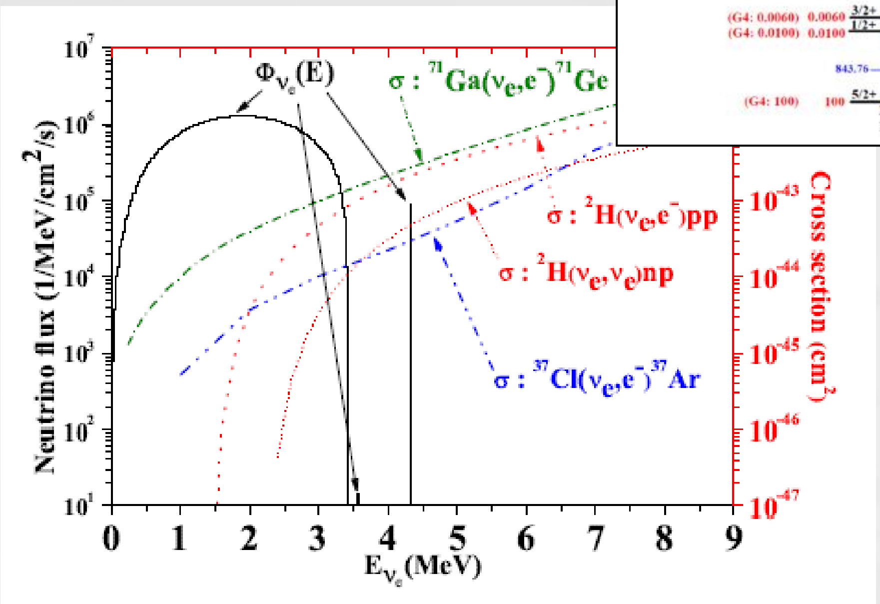


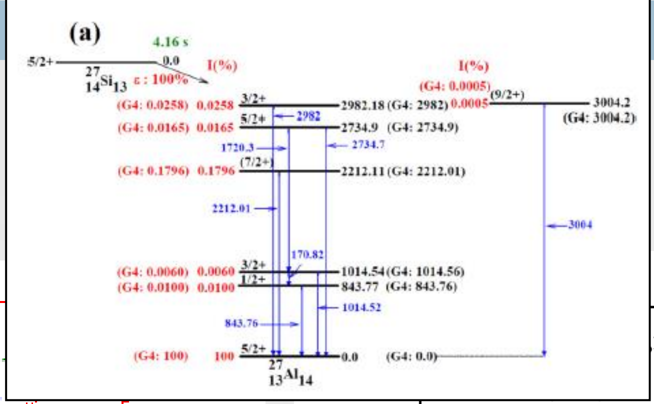


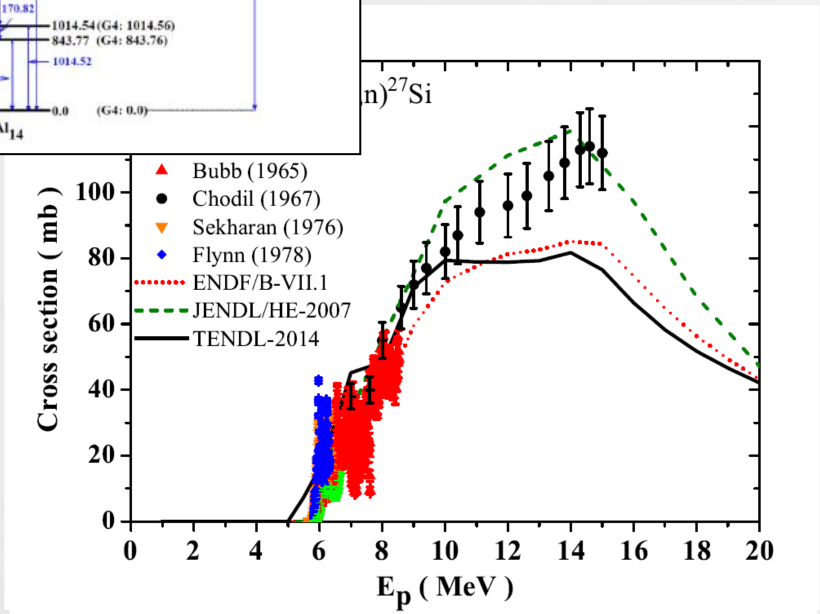


- Expected electron-neutrino energy spectrum at a distance of 10 m from the $^{27}$Al target.

-The neutrinos are generated from decay of $^{27}$Si produced by **15 MeV** and **10 mA** proton beam on a **$^{27}$Al** target.

-Theoretical cross section for $^{37}$Cl($\nu_e$,e–)$^{37}$Ar [44], $^{71}$Ga($\nu_e$,e–)$^{71}$Ge [45], $^{2}$H($\nu_e$,e–)pp [46] and $^{2}$H($\nu_e$,e)np reactions [46]

- ✓ Provide a chance to obtain **reaction rates or energy averaged cross sections for the reactions with narrow neutrino energy region**.
- ✓ This energy region **is close to the vacuum-matter transition region in the solar neutrino physics.**


[44] J. N. Bahcall, E. Lisi, D. E. Alburger, L. D. Braeckeleer, S. J. Freedman, and J. Napolitano, Phys. Rev. C 54, 411 (1996).
[45] J. N. Bahcall, Phys. Rev. C 56, 3391 (1997).
[46] S. Nakamura, T. Sato, S. Ando, T.-S. Park, F. Myhrer, V. Gudkov, and K. Kubodera, Nucl.Phys. A 707, 561 (2002).

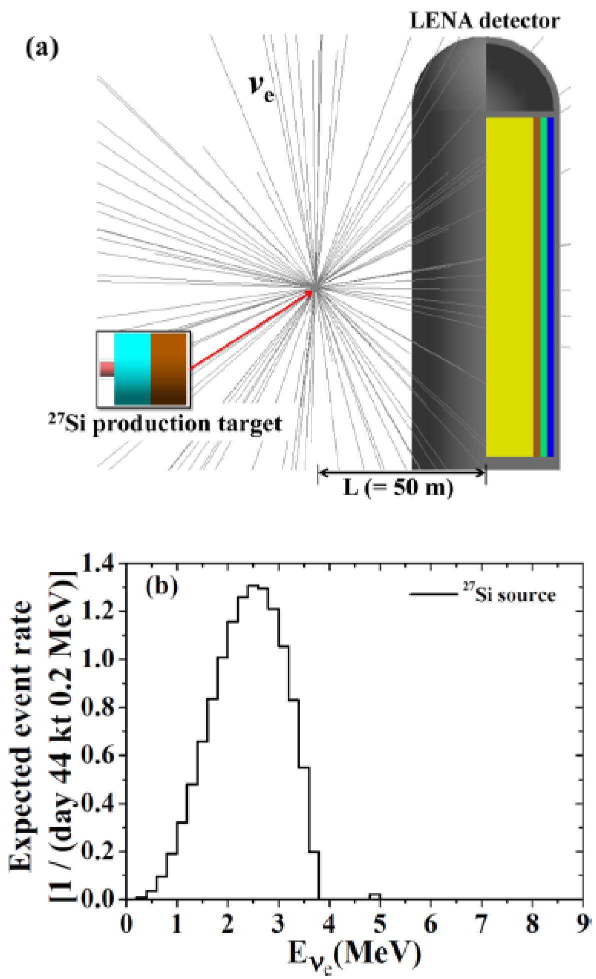


FIG. 5. Panels (a) and (b) show a simulation snapshot and expected event rates for a LENA-type detector, respectively. The neutrinos are generated from the decay of $^{27}$Si produced by the 15-MeV and 10-mA proton beams on a $^{27}$Al target. The distance between the $^{27}$Si source and the center of the LENA detector is assumed to be 50 m.

$$\frac{dR_{\nu_e}}{dT} = n_e \int_0^{E_{\max}} dE_\nu \Phi_{\nu_e}(E_\nu) P_{ee}(E_\nu) \frac{d\sigma}{dT}, \qquad (3)$$

$$\frac{d\sigma}{dT}(\nu_l e \to \nu_l e) = \frac{2G_\mu^2 m_e}{\pi E_\nu^2}\left[a^2 E_\nu^2 + b^2 (E_\nu - T)^2 - ab m_e T\right], \qquad (4)$$

$$P(\nu_e \to \nu_e) = 1 - \sin^2 2\theta_{13} S_{23} - c_{13}^4 \sin^2 2\theta_{12} S_{12}, \qquad (5)$$

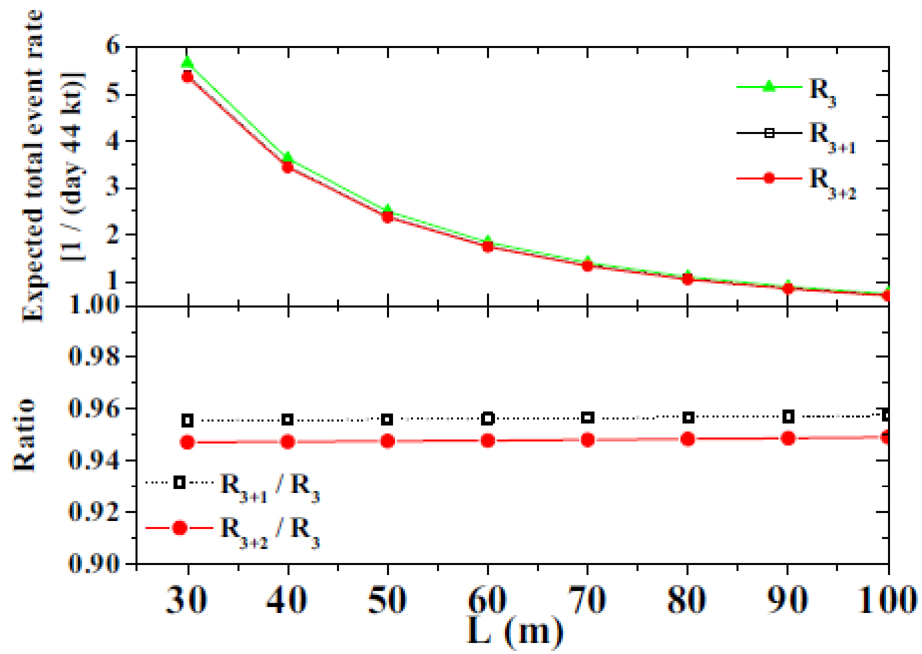


FIG. 8. Expected event rates and their ratios for LENA-type detector. The neutrinos are generated from decay of $^{27}$Si produced by the 15-MeV and 10-mA proton beams on a $^{27}$Al target. $R_3$, $R_{3+1}$, and $R_{3+2}$ are mean the reaction rates with electron-neutrino survival probabilities $P_3$, $P_{3+1}$, and $P_{3+2}$ in Eqs. (5), (6), and (7), respectively. $L$ is the distance between the $^{27}$Si source and the center of the LENA detector.

# $^{13}C + {}^{9}Be$ reaction

An electron antineutrino source by using an accelerator-based IsoDAR concept with a $^{13}C$ beam and a $^{9}Be$ target is suggested. 75 MeV/u $^{13}C$ beams with 300 p$\mu$A of current, namely 293 kW of beam power, is considered in this work.[1]

Target :R = 5cm L =10cm

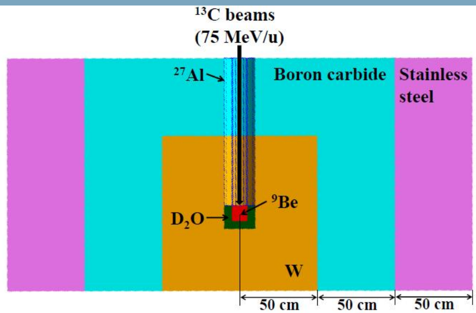


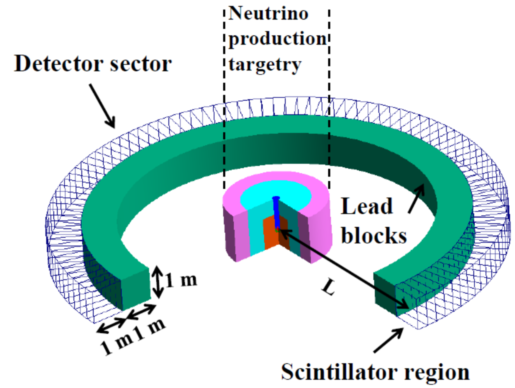


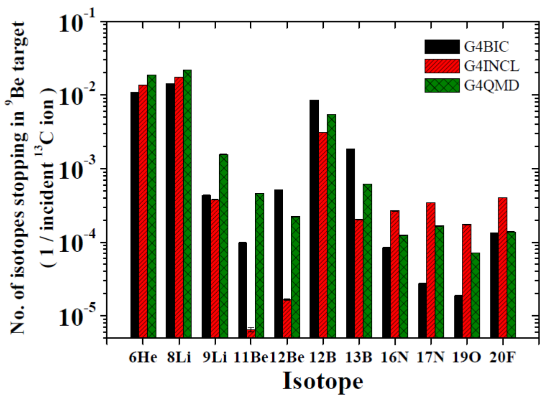


Figure 3: (Color online) Production isotope yields in $^{9}$Be target obtained from G4BIC, G4INCL and G4QMD.

For Sterile Neutrino Study

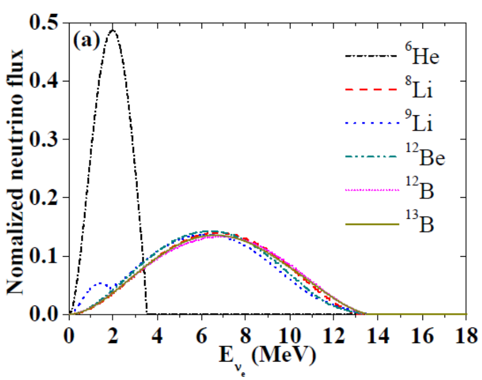


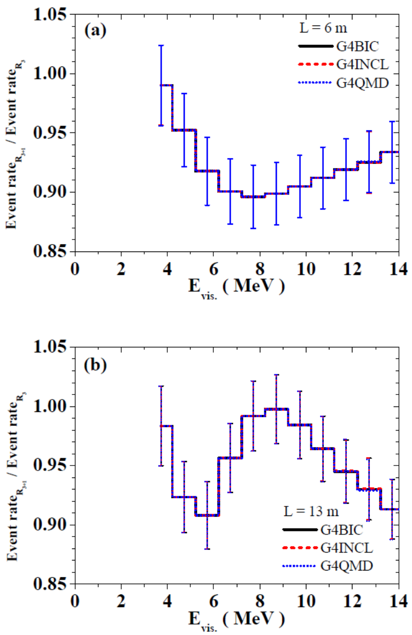


Figure 8: (Color online) Ratios of $R_{3+1}$-to-$R_3$ with respect to $E_{vis}$ at (a) L = 6 m and (b) L = 13 m are shown.

# Non-accelerator anti-neutrino source

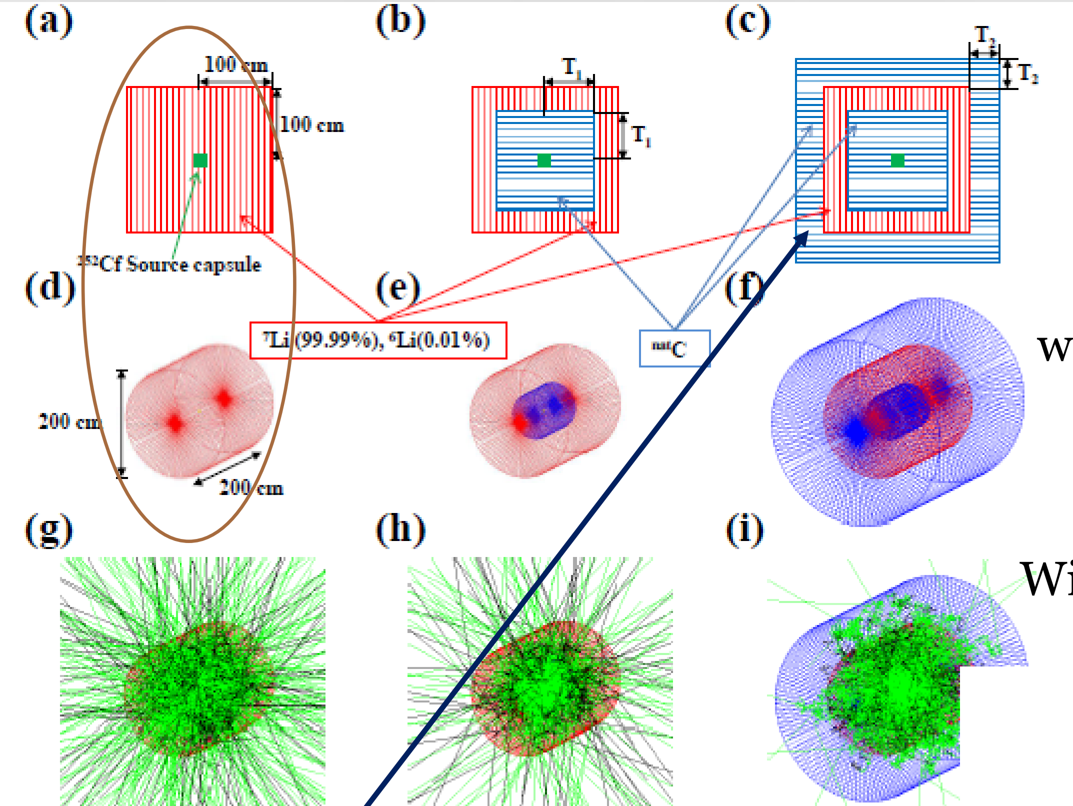


Neutron capture on $^7$Li and $^8\mathrm{Li} \rightarrow {}^8\mathrm{Be} + e^- + \bar{\nu}_e.$

w/o 252Cf

With 252CF

Carbon as neutron reflector

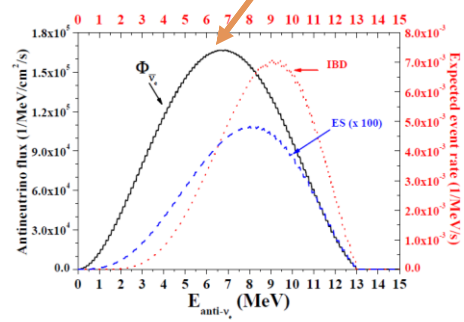


FIG. 3: (Color online) $\bar{\nu}_e$ flux from $^8$Li source and expected event rates for ES and IBD. The black solid line is the electron-antineutrino energy spectrum. The red dotted line and the blue dashed line are the event rates for IBD and ES, respectively. For ES, we multiply 100 to the rate.

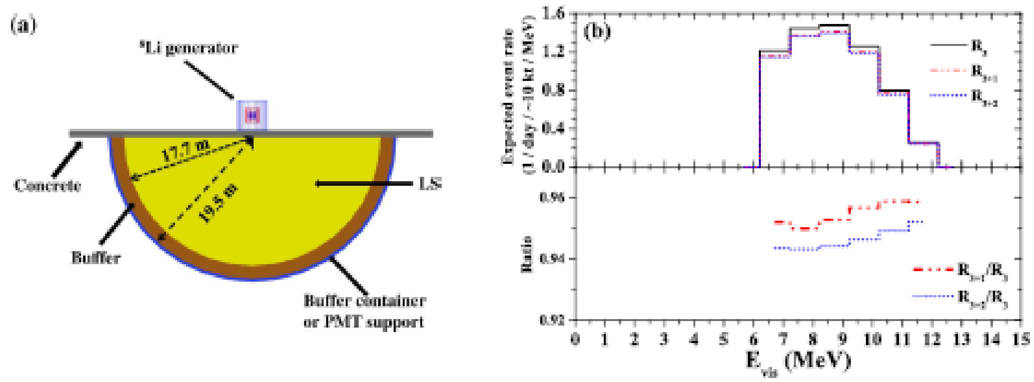


**Figure 5.** (a) OpenGL picture showing simulation geometry for hemisphere type detector with $^{8}$Li generator. (b) Expected event rates, $R_3$, $R_{3+1}$ and $R_{3+2}$ by $P_3$, $P_{3+1}$ and $P_{3+2}$ models, and their ratios with respect to $E_{vis}$. Here $6 \times 10^{11}$ $\bar{\nu}_e$ $s^{-1}$ from the setup III source with $T_1$ = 43 cm and $T_2$ = 100 cm by 1 g of $^{252}$Cf is applied for the calculation.

J. Phys. G: Nucl. Part. Phys. **44** (2017) 09LT01 Letters

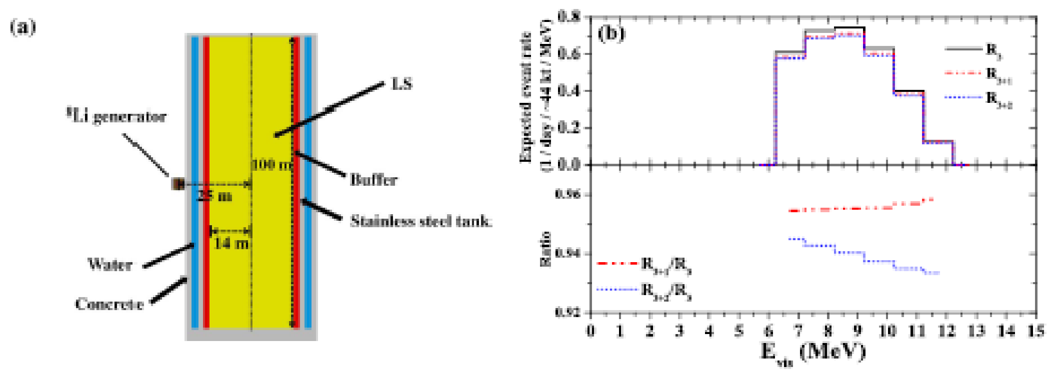


**Figure 6.** Same as in figure 5 except that the detector has a cylinder shape.

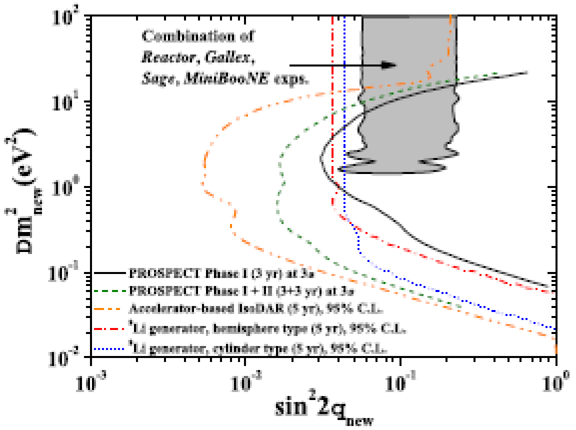


**Figure 7.** 95% C.L. sensitivity of the hemisphere and the cylinder type detector with $^{8}$Li generator proposed in this work. The gray area is an allowed region in the parameter space from the combination of reactor neutrino experiments, Gallex and Sage calibration sources experiments, and MiniBoone [4]. Sensitivities of PROSPECT (for Phase I and Phase II) [10] and an accelerator-based IsoDAR by using $^{8}$Li source [16] are also plotted.

**Table 1.** The key parameters used in this work.

| | |
|---|---|
| Neutron source | $^{252}$Cf |
| Neutron intensity | $2.34 \times 10^{12}$ n s$^{-1}$ g$^{-1}$ |
| Neutrino production target | $^{7}$Li (99.99% enhanced) surrounded by graphite |
| Run period | 5 years |
| $\bar{\nu}_e$/neutron | 0.256 |
| $\bar{\nu}_e$ flux | $6 \times 10^{11}$ $\bar{\nu}_e$ s$^{-1}$ g$^{-1}$ |
| Neutrino energy cut | 7 MeV ($E_{\rm vis} = 6.22$ MeV) |

| Detectors | Hemisphere type | Cylinder type |
|---|---|---|
| Fiducial mass | 10 kt | 44 kt |
| IBD event total | 9750 | 4960 |

# Thanks for your attention !

**- 1 g of Isotope seems to be a large source (micrograms is the usual unit), on a similar scale to the SOX source. What are the issues with making and transporting the source? These were non-trivial for CeLAND and are the reason that SOX in Italy and not CeLAND in Japan is moving forward**.

Reply:
If a reprocessing facility is located at outside of the country in which a neutrino detector exists, the transporting of radioisotopes is an important problem as suggested by the referee 2. The possible quantity transported by an air plane is very low. When the quantity of a radioisotope source is high, it should be slowly transported by sea boat. Because the half-life of 252Cf is as long as 2.6 y, the decay of 252Cf during a several ten days in transport is small. Thus, it is practically possible to transport a 252Cf source by sea.

The production of radioactivity is another problem. 144Ce is chemically separated from spent nuclear fuels in a reprocessing facility. The peak of yields of fission products of actinides such as 235U are approximately A=95 and 130. Because A=144 slightly differs from A=135, the fission yield of 144Ce is 5.2%, not so high. Furthermore, 144Ce decays out during the reprocessing and transport with a half-life of 284 day. Thus, the possible quantity of 144Ce is limited by its fission yield and half-life.

Main problem in CeLAND is to shield in the transport because of the 2.186 MeV gamma radiation with 0.7% branching ratio. The 75kCi 144Ce for CeLAND needs heavy tungsten shield in the transport and makes the non-trivial burden in the transportation.

In contrast, 252Cf is generated from actinide materials by successive neutron capture reactions in high flux nuclear reactors. In this case, the production rate is approximately proportional to the quantity of target materials and the neutron radiation time. Because the half-life of 252Cf is as long as 2.6 y, it is possible to irradiate for several years. Thus, 252Cf production is easier than 144Ce production and transportation.

There is no explicit necessary reason to produce and transport 1 g of 252Cf isotope in our idea. For example, we may divide the 1g of 252Cf isotopes into a tenth part (0.1 g) and can transport each part. And each isotope can be placed near the center of inner graphite as a cluster type source, which scheme does not make the 8Li yields much different from the present situation.

**- 252Cf seems to produce some gamma radiation. Can this be neglected in this analysis or is shielding included? How would shielding affect the deployment of the source?**

Reply: The IBD reactions exploited in the present work offers two distinct signals comprising a prompt signal due to an annihilation of a positron and a delayed signal of a 2.2 MeV gamma ray following a neutron capture. We expect that the coincidence method using the IBD reactions provides almost unambiguous antineutrino event detection and gives an efficient rejection of other possible backgrounds. Furthermore, because we use the neutrino energy cut of 7 MeV (corresponding to E_vis = 6.22 MeV), we expect that the effect of low energy gammas is not large.

Second, in order to decrease possible pile-up effects and accidental events, additional radiation shields can also be considered in our setup without much difference from 8Li yield of the present case. For example, additional shield structure for hemisphere type detector can be installed on our system (see Fig. 1 and Fig.5 in the revised manuscript).

A lead shield with a thickness of 50 cm can be considered to be located outside of this graphite (T2=50 cm), but 8Li production region is not changed. In addition, the combination of a concrete shield with a thickness 30 cm and another lead shield with a thickness with 70 cm is considered between 8Li generator and scintillator detectors. Consequently, 120 cm of Pb and 30 cm of concrete shielding can be constructed for shielding the gamma radiation.

Also, there may be additional gamma-ray backgrounds from the Pb shield (or tungsten), but which may have energies below the energy cut used in this work. Higher energy gammas (< 10 MeV) are reduced well by the above shields. For example, for 8 MeV gamma-rays with the 120 cm of Pb and 30 cm of concrete shields, its intensity can be shown to be decreased by a factor < 10-28 by using exponential attenuation law accounting for Compton scattering and photoelectric effect from Ref.[ https://www.nist.gov/]. Of course, tungsten shield instead of lead can be more effective than lead shield. Note that these shields do not affect the penetration of neutrinos.

**- 252Cf is heat production an issue from the neutron and gamma radiation? Will it need to be cooled? Once again, how would this affect the deployment of the source?**

Reply: First, the heat of a 252Cf source with 1.0 g is approximately 38.7 W. The cooling of 38.7 W is easy. This is very smaller than those from the 144Ce-144Pr source with 50 kCi (~370 W) in Ref. [Cribier et al. Phys.Rev.Lett., 107 (2011) 201801] and the proton accelerator IsoDAR (600 kW) in Ref. [Bungau et al. Phys.Rev.Lett. 109 (2012) 141802]. Second, in our design, because the 252Cf source is located outside of the detector, the cooling of the neutrino source is easy. Moreover, if we need, we make the source in several pieces of the 252Cf which can be distributed in the graphite materials. We also install other cooling arrangement inside the graphite, if needed.

$1\ \mathrm{Ci} = 3.7 \times 10^{10}\ \mathrm{Bq} = 37\ \mathrm{GBq}$

and

$1\ \mathrm{Bq} \cong 2.703 \times 10^{-11}\ \mathrm{Ci} \cong 27\ \mathrm{pCi}$